IEEE Access
Multidisciplinary | Rapid Review | Open Access Journal

Received December 23, 2019, accepted January 15, 2020, date of publication January 28, 2020, date of current version February 5, 2020.

Digital Object Identifier 10.1109/ACCESS.2020.2970084

Suppression of Speckle Noise in Digital Holography With Spatial and Temporal Domain Depolarization

TONGYAO DU, YONG KONG, XINLEI QIAN, WEI DING, AND ZHENWEI WANG
School of Electronic and Electrical Engineering, Shanghai University of Engineering Science, Shanghai 201620, China

Corresponding author: Yong Kong (kkyy7757@163.com)

This work was supported by the Natural Science Foundation of Shanghai under Grant 19ZR1421700.

ABSTRACT Speckle noise in digital holography has a great influence on image quality, and one of the reasons for the formation of speckle noise is that the degree of coherence for the reference light and the object light is too high and unnecessary noise is introduced to the recorded hologram. In this paper, the spatial depolarization and the temporal domain depolarization are analyzed to reduce the speckle noise. The spatial depolarization utilizes the depolarization performance of the depolarizer. By adding a quartz depolarizer to the object light, the linearly polarized light in the object light becomes randomly polarized light, thereby reducing the degree of coherence with the reference light, realizing the suppression of speckle noise, and by utilizing the characteristics of pupil parameters towards the depolarization degree, it is to realize the control for the degree of coherence. The temporal domain depolarization uses two quarter-wave plates and adjustable liquid crystal to realize the depolarization superposition. By controlling the phase delay of the liquid crystal phase variable retarder, the multi-depolarization accumulation in a short time is realized, and the experimental results show that this method preserves the detail portion of the image while better removing speckle noise. Finally, the Non-Local Means filtering algorithm is used to make the reconstructed image smoother. The method proposed in this paper has great applicable value for improving the image quality of digital holography system.

INDEX TERMS Digital holography speckle noise, depolarization, quartz depolarizer, liquid crystal.

I. INTRODUCTION

Digital holography has been widely used in various fields. It contains a large amount of information and has a large practical value, but it also has shortcomings. There are large speckle noises in the recorded digital holographic images, which leads to some image quality being poor and will have certain influence on the practical application [1]–[3]. Therefore, many scholars are also studying to reduce the coherence of the light source with various methods to suppress speckle noise, such as multi-mode fiber or multi-beam fiber coupling to provide a light source [4]. Reducing the coherence of the light source by a motion scatterer or a phase shifter [5], and a low-coherence light source or white light [6] is used as a light source, and using a combination of the above methods [7]. Multi-wavelength recording holograms are used to eliminate speckle noise [8], but this method is complicated to process. A method of rotating a ground glass piece [9] is added to the interference system to reduce the coherence of the light source. Practice has shown that the use of rotating frosted glass sheets can reduce the diffraction noise of the system [10]. The spatial resolution of the system is improved due to the reduced self-coherence length. Introducing a rotating frosted glass sheet into photorefractive holography to remove speckle noise from the system [11] and introduce the frosted glass sheet into a digital holographic microscope to improve the observation resolution of biological samples [12]. In addition, the noise can be processed by an algorithm, and the image is processed by median filtering [13] which leads to partial loss of detail. A pixel separation method has been proposed [14], [15], but this method does not suppress periodic interference noise. It is proposed to effectively suppress such coherent noise by using optical scanning multi-view method combined with 3D

The associate editor coordinating the review of this manuscript and approving it for publication was Joewono Widjaja.

block matching numerical filtering [16], this method takes a long time to scan and calculate. An optimization method combining two-dimensional empirical mode decomposition and dual-wavelength digital holographic microscopy is proposed to improve the imaging quality [17], however, its scope of application is limited. A complex amplitude field reconstruction scheme based on noise robust pixel super-resolution multi-image phase retrieval algorithm is proposed [18], which does not involve the influence of polarization state. By rotating the polarization direction, the diversity of polarization can effectively reduce speckle noise. However, the method of changing the polarization direction requires the polarization state to rotate more than 20 degrees to ensure that the holograms are not related to each other. Therefore, this method can not obtain a large number of decorrelation holograms, and the image quality improvement method of the reconstructed image is limited. A kind of triangular mesh hologram uses different staggered plane carrier sets to generate multiple holograms and display them in time multiplexing order to eliminate speckle artifact [19]. But the calculation time of this method is too long. Another method is to use programmable filter in general 4-f optical structure through digital micro mirror array device. Through selective filtering of spectrum component [20], speckle noise can be effectively reduced.This method requires additional camera equipment, which leads to complex system structure. The laser illumination system of multimode fiber bundle can also be used to reduce speckle noise [21].However, the correlation length of the incident laser beam increases by a factor equal to the magnification of the optical system. Another method is to use a piezoelectric transducer with multimode fiber [22], the dynamically modulated fiber structure produces a time average smoothing effect on the output field distribution in a short time to reduce speckle. For the method of reducing the degree of coherence, some researchers increase the fiber between the laser and the medium. This method can effectively reduce the degree of coherence of the light source. [23]. A polymer film speckle scrambler can also be used to reduce the effect of coherence [24]. The spatial coherence of the laser can also be reduced by rotating the diffuser in a multi-path system [25]. The speckle free quantitative phase imaging is realized by using the common optical path Fresnel biprism interferometer. Some researchers also synthesize a pseudo thermal light source to realize partially coherent light source [28], which can illuminate the sample uniformly to reduce the effect of speckle noise.

II. THEORETICAL ANALYSIS AND SIMULATION

A. SPECKLE NOISE ANALYSIS

Digital holography is a hologram obtained by recording interference images of reference waves $O(x, y)$ and object waves $R(x, y)$ by the principle of interference. The total light intensity of CMOS recording is given as follows:

$$\begin{aligned} I_H(x,y) &= |O(x,y) + R(x,y)|^2 \\ &= OO^* + RR^* + OR^* + O^*R \end{aligned} \tag{1}$$

Using the principle of holographic diffraction reproduction, the image is reconstructed by computer, and the image is restored by the conjugate light of the reference light, and the reproduction light of hologram is expressed as follows:

$$\begin{aligned} U_C(x,y) &= C(x,y)\, I_H(x,y) \\ &= COO^* + CRR^* + COR^* + CO^*R \end{aligned} \tag{2}$$

where COR^* contains the wavefront information of the object, but the holographically recorded light source has a high coherence, which makes the light wave have different scattering effects on different objects when it is reflected on the surface of the object. A speckle pattern develops if the height variations of the rough surface are larger than the wavelength of the light, Speckles result from interference of light scattered by the surface points. The phases of the waves scattered by different surface points fluctuate statistically due to the height variations. If these waves interfere with each other, a stationary speckle pattern develops. Moreover, most of the recorded objects are rough objects. The surface of the rough object is equivalent to a variety of reflection elements that react differently to the beam. Random phase elements are added to the reflected light field, and these random phase elements interact with each other to produce a set of random phases. For these random phases, the transmittance of the object is discussed as follows:

$$t(r) = f(r)\, n(r) \tag{3}$$

where $f(r)$ is the object information in the ideal state , $n(r)$ is the random phase carried. Set the reflectivity of the object to be $f(x_0, y_0, z_0)$, the object wave can be represented as follows:

$$\begin{aligned} &O(x,y) \\ &= \sum f(x_0,y_0,z_0)\, n(x_0,y_0,z_0) \exp[i\frac{2\pi}{\lambda} n(x_0,y_0,z_0)] \end{aligned} \tag{4}$$

where $\frac{2\pi}{\lambda} n(x_0, y_0, z_0)$ is a random phase difference due to the undulations on the surface of the object itself. Then the conjugate image of the object reproduced by the hologram can be expressed as follows:

$$\begin{aligned} &E(x,y) \\ &= A' \sum f(x_0,y_0,z_0)\, n'(x_0,y_0,z_0) \exp[i\frac{2\pi}{\lambda} n'(x_0,y_0,z_0)] \end{aligned} \tag{5}$$

the intensity of the conjugate image is expressed as follows:

$$\begin{aligned} I &= E(x,y)\, E^*(x,y) \\ &= A'^2 \sum |f(x_0,y_0,z_0)|^2 \left| n'(x_0,y_0,z_0)^2 \right| = \beta I_0 I_n \end{aligned} \tag{6}$$

where I_0 is the ideal object light intensity and I_n is the speckle intensity.

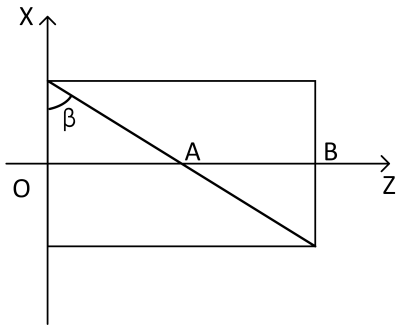

FIGURE 1. Quartz depolarizer structure.

B. SPATIAL DOMAIN DEPOLARIZATION ANALYSIS

From the analysis of the previous section, it is possible to obtain a large amount of speckle caused by light wave scattering due to the high coherence degree of the light source and the roughness of the object surface, and finally the holographic surface is imaged. When the image is reconstructed, the speckle is modulated by the diffraction calculation of the holographic fringes to each diffraction order, so that speckle noise appears on the reconstructed image, and the quality of the image is lowered. Therefore, the speckle noise can be reduced by reducing the coherence degree of the two interfering beams. Therefore, the use of a quartz depolarizer in the object light can effectively reduce the coherence degree. The characteristics of the depolarizer are analyzed below.

The structure of the quartz depolarizer is shown in Fig. 1. It is composed of two left and right spin quartz crystals with the same structure angle. The spinning properties of the two quartz crystals must be opposite.

In the Fig. 1, β becomes the structural angle, Z axis is the optical axis' propagation direction, and O is the center of the pupil; let an electric vector get through the left side length of the crystal OA $= d_1$ and get through the right side length of the crystal AB $= d_2$. Since the light propagates along the optical axis in the depolarizer, the depolarizer acts as a activizer, and its Mueller Matrix can be expressed as:

$$\boldsymbol{M} = \begin{bmatrix} 1 & 0 & 0 & 0 \\ 0 & cos2\varphi & sin2\varphi & 0 \\ 0 & -sin2\varphi & cos2\varphi & 0 \\ 0 & 0 & 0 & 1 \end{bmatrix} \tag{7}$$

where $\varphi = \alpha L$ is the optical rotation angle, α is the optical rotation power of the substance

The numerical value is related to the wavelength $\alpha = \frac{\Delta n}{\lambda}\pi$, Δn is the birefringence of quartz and λ is the wavelength, L is the distance of light passing through the quartz crystal.

Since the depolarization effect of this property is realized in the spatial, the average Mueller Matrix for $\boldsymbol{M}$ is first obtained by integrating in the pupil range $\bar{\boldsymbol{M}} = \int_{\sum} \boldsymbol{M} dxdy$.

For $cos2\varphi$ and $sin2\varphi$ there are integrals in the range of the pupil, which are expressed as follows:

$$\begin{cases} (cos2\varphi)_{\sum} = \frac{1}{\pi}\int_{\sum} \cos(fx+b)\, dxdy = 2cosb\frac{J_1(f)}{f} \\ (sin2\varphi)_{\sum} = \frac{1}{\pi}\int_{\sum} \sin(fx+b)\, dxdy = 2sinb\frac{J_1(f)}{f} \end{cases} \tag{8}$$

where $b = 2\alpha(d_1 - d_2)$, $J_1(f)$ is a first-order Bessel function. Then the Mueller Matrix of the depolarizer can be expressed as follows:

$$\bar{\boldsymbol{M}} = \begin{bmatrix} 1 & 0 & 0 & 0 \\ 0 & 2cos\frac{J_1(f)}{f} & 2sinb\frac{J_1(f)}{f} & 0 \\ 0 & -2sinb\frac{J_1(f)}{f} & 2cos\frac{J_1(f)}{f} & 0 \\ 0 & 0 & 0 & 1 \end{bmatrix} \tag{9}$$

When the included angle between the polarization direction of the incident beam polarization and the X-axis is θ, Let $\boldsymbol{S}_{in}, \boldsymbol{S}_{out}$ represent the Stokes vector of the input and output beams, respectively, then $\boldsymbol{S}_{out}$ is expressed as follows:

$$\begin{aligned} \boldsymbol{S}_{out} &= \bar{\boldsymbol{M}}\boldsymbol{S}_{in} \\ &= \begin{bmatrix} 1 & 0 & 0 & 0 \\ 0 & 2cos\frac{J_1(f)}{f} & 2sinb\frac{J_1(f)}{f} & 0 \\ 0 & -2sinb\frac{J_1(f)}{f} & 2cos\frac{J_1(f)}{f} & 0 \\ 0 & 0 & 0 & 1 \end{bmatrix} \begin{bmatrix} 1 \\ cos2\theta \\ sin2\theta \\ 0 \end{bmatrix} \\ &= \begin{bmatrix} 1 \\ 2\cos(b - 2\theta\frac{J_1(f)}{f}) \\ -2sin(b - 2\theta\frac{J_1(f)}{f}) \\ 0 \end{bmatrix} = \begin{bmatrix} S_0 \\ S_1 \\ S_2 \\ S_3 \end{bmatrix} \end{aligned} \tag{10}$$

It can be seen from Eq. 10 that after a linearly polarized beam of a certain section is perpendicularly incident on the quartz depolarizer, because each incident point passes d_1, d_2 differently, the emergent light will get mixed light with different electric vector vibration directions, achieving the effect of depolarization, and at the same time achieving the purpose of reducing the degree of coherence.

The degree of polarization for the emergent light can be obtained by the definition of the degree of polarization:

$$\begin{aligned} P &= \frac{(S_1^2 + S_2^2 + S_3^2)^{1/2}}{S_0} = 2\left|\frac{J_1(f)}{f}\right| \\ &= 2\left|\frac{J_1(4\frac{\Delta n}{\lambda}\pi R tan\beta)}{4\frac{\Delta n}{\lambda}\pi R tan\beta}\right| \end{aligned} \tag{11}$$

It can be seen from Eq. 11 that for one-wavelength laser and a certain quartz depolarizer, λ, Δn, β are certain, the degree of depolarization depends on the pupil radius R. The numerical calculation for the relationship between the pupil radius R and the depolarization degree is shown in Fig. 2. By changing the polarization state emitted from the

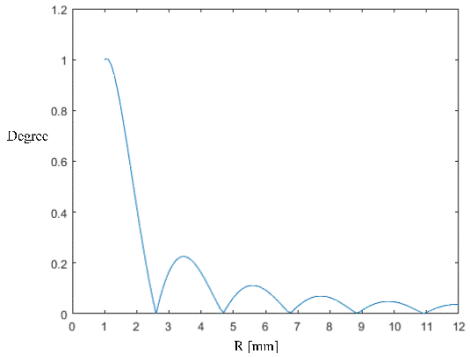

FIGURE 2. Relationship between Degree of polarization and pupil radius R.

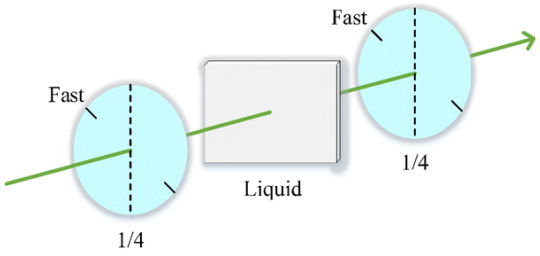

FIGURE 3. Temporal domain depolarization module structure.

object light beam, it can achieve different degrees of coherence with the reference light and achieve spatially adjustable degree of coherence.

C. TEMPORAL DOMAIN DEPOLARIZATION ANALYSIS

The temporal domain depolarization realizes the variable phase delay by adjusting the signal input of the liquid crystal, and in combination with the front and back two 1/4 wave plates, it is to form a temporal domain depolarization module, as shown in Fig. 3, when a beam of linearly polarized light is incident perpendicularly on the 1/4 wave plate, the included angle between the polarization direction of the incident beam polarization and the fast axis of the wave plate is 45°, and the light beam is decomposed into two components which are the fast axis and the slow axis vibrations. The phase amplitudes are all equal, $|E_r| = E_0\cos\theta = |E_s| = E_0\sin\theta = \sqrt{2}/2E_0$.

When the liquid crystal is loaded by the swept-frequency signal, the emitted light produces a phase retardation amount of δ. At this time, the two vibration components are given as follows:

$$\begin{cases} E_r = \dfrac{\sqrt{2}}{2}E_0\sin(\tau+\delta) \\ E_s = \dfrac{\sqrt{2}}{2}E_0\sin\tau \end{cases} \tag{12}$$

Liquid crystal is a kind of positive and single axis photoelectric material, which has the characteristics of changing the potential energy of molecules to the lowest state, and the characteristics of forced orientation arrangement of external electric field [27]. When the potential energy of the liquid crystal molecule is the lowest, it means that the direction of the liquid crystal molecule is the same as that of the field line of the external electric field. Fig. 4 is Fresnel's refractive index sphere, in which $n_x = n_y = n_0$ (ordinary light refractive index), $n_z = n_e$ (unusual light refractive index, and there is $n_e > n_o$)z axis is the optical axis (symmetry axis), k_0 is the beam direction, and the plane with k_0 as the normal cuts the curve l through the center of the refractive index ellipsoid. In the liquid crystal molecule, the optical axis direction is the long axis direction of the molecule. Therefore, when a beam of light is incident on the liquid crystal molecule, the polarization direction of the outgoing light can be determined according to its incident angle and polarization direction.

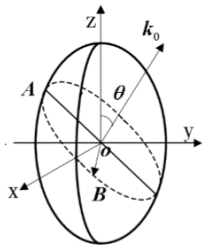

FIGURE 4. Refractive index ellipsoid of liquid crystal.

If the beam k_0 is parallel to the z-axis, the curve l is circular in the $x-y$ plane, and the refractive index of a liquid crystal is n_0, and the polarization direction of the incident light will not change after passing through the liquid crystal.

If the beam k_0 is incident along the x-axis, then the curve L is an ellipse on the $y-z$ plane, its short axis is n_0, and its long axis is n_e. After the incident light passes through the liquid crystal, due to the difference between the x-axis and the y-axis direction, it will become elliptical polarized light.

If there is an angle θ between the k_0 and z axes of the incident light, then the curve l is an ellipse on the inclined plane, its short axis is n_0 and its long axis is n_{eff}. The formula is as follows:

$$n_{eff}(\theta) = \frac{n_o^2 n_e^2}{n_e^2\cos^2\theta + n_o^2\sin^2\theta} \tag{13}$$

where $n_o < n_{eff}(\theta) < n_e$, the polarization direction of the incident light will be changed after passing through the liquid crystal.

When the frequency of the applied electric field changes, the dielectric constant of the liquid crystal will change. At the same time, these changes will cause the change of birefringence in the liquid crystal layer. Thus, as shown in formula (12), when light propagates along the liquid crystal, the phase difference δ gradually increases. Non linearly polarized light after depolarization is formed by superposition of components in two directions.

After loading different signals on the liquid crystal, different phase delay amounts δ can be obtained. When passing through the 1/4 wave plate again, the component propagation speed on the fast axis is faster, and the components in

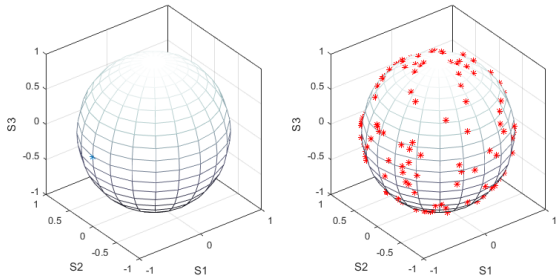

FIGURE 5. Polarization diagram of Poincare sphere.

the two directions are superimposed to form non-linearly polarized light after the depolarization.The signal generator is used to frequency sweep the liquid crystal, in order to continuously change the phase delay amount generated by the liquid crystal, so that the linear polarization achieves different depolarization effects in the temporal domain. The polarization state of incident light and emergent light can be simulated by the Poincare sphere as shown in Fig. 5.

What is different from the spatial domain depolarization is that, the polarization state in this mode is always in a state of change, and various types of depolarization patterns are recorded, and the obtained information is more comprehensive. Based on the statistical characteristics of speckle noise, the holograms recorded in multiple polarization states have independent speckle noise, and the holograms recorded after sweeping is expressed as follows:

$$I = \beta I_0 \left(I_1 + I_2 + \ldots + I_m\right) = I_0 I' \tag{14}$$

where I_0 is the ideal object light intensity, β is the average coefficient, $I_1, I_2 \ldots I_m$ are independent of the multiplicative speckle noise, I' is the averaged speckle noise, which can be known by the principle of non-coherent superposition. The speckle effect of the hologram will be weakened.

This experimental system does not require additional mechanical operation, the liquid crystal responds quickly, and the depolarization effect can be achieved by adjusting the input signal of the signal generator, and the error generated for the entire optical system is negligible.

III. EXPERIMENT AND RESULTS

The off-axis optical path of the experimental light path is shown in Fig. 6(a) and 5(b), where in Laser is a laser light source with a wavelength of 532 nm; PBS is a polarizing beam splitter, which acts as a beam deflection; M1, M2 are plane reflectors; BS is a beam splitter; ND is an optical rotating gradient sheet for adjusting the intensity of reference light; BE1, BE2 are beam expansion collimation modules, the objective lens size is 10×, the aperture size is 20um; and the DQ used for spatial depolarization is a quartz depolarizer. The temporal domain depolarization uses two 1/4 wave plates and a liquid crystal wave plate Liquid; CMOS is used to record holograms with a pixel of 1280×1022 and each pixel has a size of 5.3×5.3 (um); Object is a dice with a length, width and

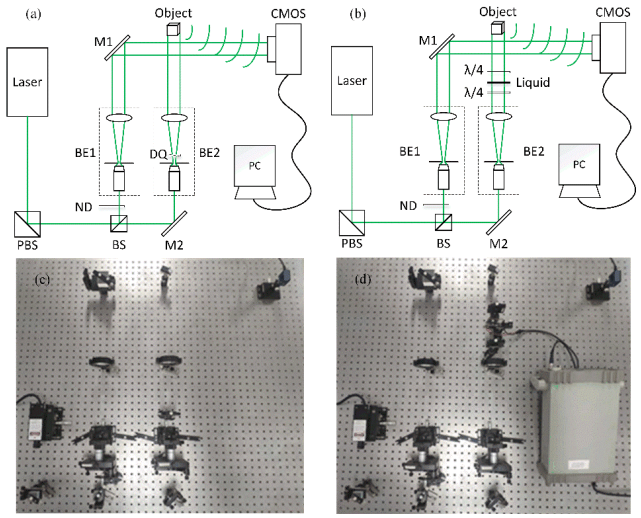

FIGURE 6. Experiment system (a) Spatial domain depolarization experiment system,(b) Temporal domain depolarization experiment system and (c),(d) is physical light path of (a) and (b).

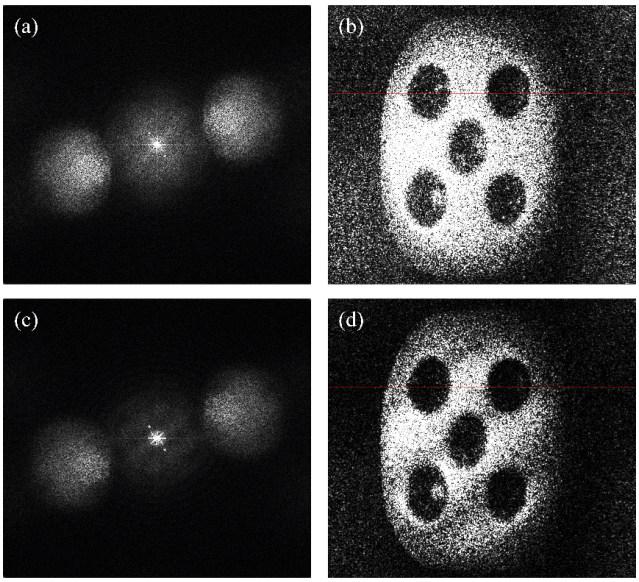

FIGURE 7. Frequency domain image and reconstructed image (a) traditional system recording hologram frequency domain image and (b) object original reconstruction image,(c) spatial depolarization system recording hologram frequency domain image and (d) object final reconstruction image.

height of 10 mm equally. The recording distance is 0.45 m, and the included angle between the reference light and the object light is 5°. The PC is a workstation-level computer, and the corresponding physical light path diagram is shown in Fig.5(c) and 5(d).

Firstly, the original hologram in the absence of quartz depolarizer is recorded by the optical path of the spatial. The spectrum is calculated by PC as shown in Fig. 7(a). The image of the object is reconstructed by the angular spectrum method as shown in Fig. 7(b). Since the reconstructed image carries strong speckle noise, an equivalent number of looks (*ENL*)

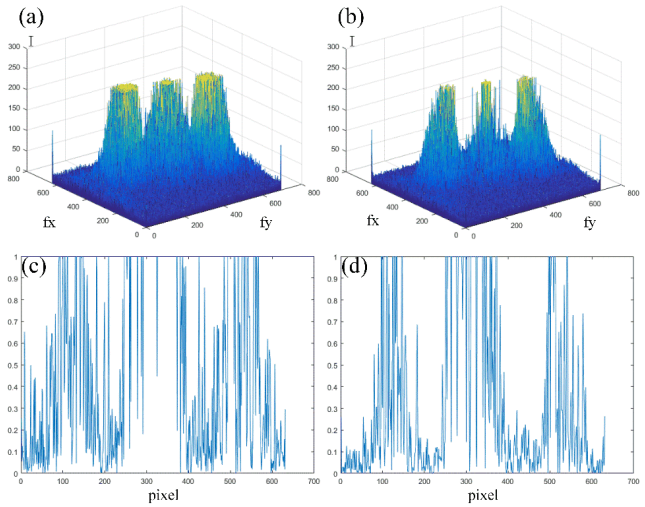

FIGURE 8. 3D display in frequency domain and normalized values of pixels (a) and (b) is 3D display of Fig. 7(a) and (c),(c) and (d) is normalized value of red section pixels of Fig. 7(b) and (d).

is introduced as a criterion for determining image quality as follows:

$$ENL = (\frac{mean}{sta})^2 \tag{15}$$

where *mean* is the mean value of the pixel size of the image, *sta* is the standard deviation. *ENL* is an index to measure the relative intensity of the speckle noise of an image. The larger the *ENL*, the more obvious the speckle noise and the worse the overall image quality.

It can be seen from Fig. 2 that the depolarization effect is very obvious when the pupil radius is greater than 5 mm. Therefore, when the depolarizer is added to the optical path, which makes the illumination spot radius greater than 5 mm, and then the hologram after the height depolarization is recorded, and the spectrum is obtained after the processing. The spectrogram and reconstructed image obtained after processing are shown in Fig. 7(c) and (d). The ENL for Fig. 7(b) and (d) are calculated to be 0.7204 and 0.9998 respectively. From the results of ENL and Fig. 7(c) and (d), the quality of the reconstructed image after depolarization is significantly better than the original reconstructed map, and the edges of the image are also clearer.

From the aspect of frequency analysis, the spectrum diagrams of Fig. 7(a) and (c) and the spectrum Fig. 8(a) and (b) after visualization three-dimensional processing, it can be seen that there is a large crosstalk among the zero-order item, the object item and the conjugate item in the frequency domain of the hologram recorded without the depolarizer, which will bring a larger speckle noise to the reconstructed image, however, the interference among the three items in the frequency domain of the hologram recorded by the depolarizer is significantly reduced, and the influence brought about by the reconstruction is smaller; secondly, it can be seen from the section lines Fig. 8(c) and (d) of the reproduced

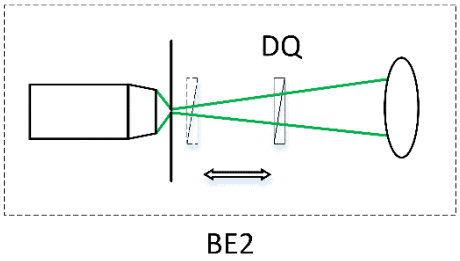

FIGURE 9. Quartz depolarizer micro-displacement.

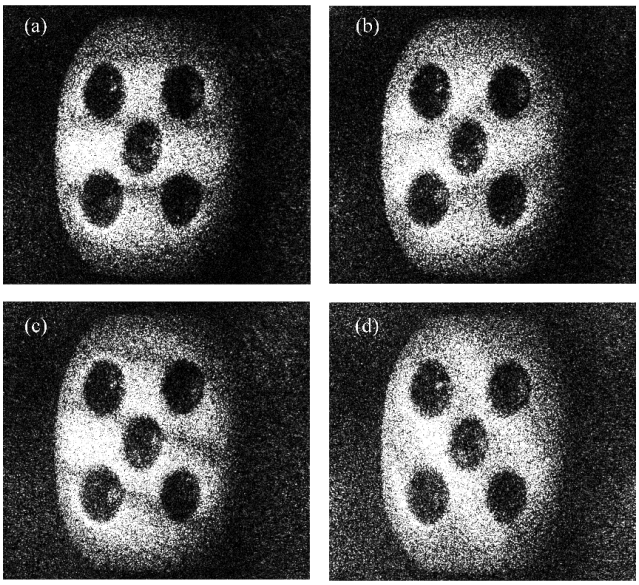

FIGURE 10. Reconstructed image with sequential micro-displacement.

object image that the latter has less noisy points and the pixel distribution is more uniform, and a certain denoising effect is obtained.

From the above results, it can be concluded that the addition of the depolarizer in the object light path has a significant inhibitory effect on the speckle noise, and different degrees of coherence have different effects on the speckle suppression effect, the relationship characteristics between the pupil radius and the degree of depolarization of the quartz depolarizer can be used to achieve different degrees of coherence. In practical applications, it has very high adaptability to situations requiring different degree of coherence and has simple structure. Therefore the experimental analysis has been done for this characteristic, on the basis of the above structure, the quartz depolarizer is slightly displaced, as shown in Fig. 9.

After the above experiment, the micro-displacement operation of the depolarizer is performed, and the pupil radius is gradually reduced. The fractionatedly recorded hologram is analyzed, and 5 results from the maximum pupil radius to the minimum pupil radius are recorded, the corresponding reconstructed images are shown in Fig. 10. *ENL* of the reconstructed map is calculated separately in contrast with the *ENL* of the original reconstructed map, as shown in Table 1. From

TABLE 1. ENL of reconstructed image.

Img.	final	a	b	c	d	original
ENL	0.7204	0.7344	0.7907	0.8594	0.9741	0.9998

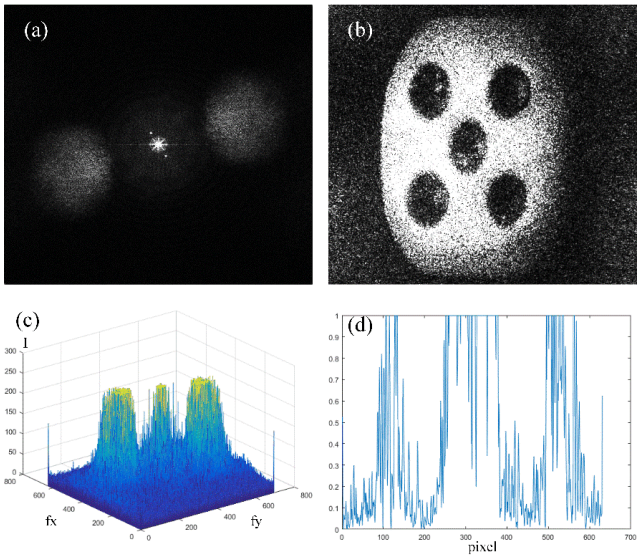

FIGURE 11. Temporal domain depolarization processing image (a) Frequency domain image of temporal domain depolarization system, (b) Reconstruct image, (c) 3D display of (a) and (d) is normalized values as in the same line position as in Fig. 7.

the results, it can be seen from the results that after the pupil radius is sequentially reduced, the *ENL* of the reconstructed image also increases with it, and the speckle noise increases. The essential reason is that the depolarization effect is also reduced due to the reduction of the pupil radius, resulting in an increase in the degree of coherence. Speckle noise is generated due to higher degree of coherence, which degrades image quality, which is consistent with previous theoretical analysis. Therefore, the structure of the adjustable coherence degree is advantageous for studying objects of different materials.

The above analysis can achieve the denoising effect of the reconstructed image obtained by the depolarizer achieving the spatial depolarization, and the depolarizer has different degrees of denoising effect corresponding to different positions. Then the optical path is adjusted to the temporal domain depolarization optical path for shooting and recording, the output of the signal generator is connected to the positive and negative poles of the liquid crystal wave plate, turn on the sweep frequency function, set the 5V sinusoidal carrier. The frequency range is set to 1 kHz to 10 kHz continuous sweep-frequency, the scan time is 10 seconds, and the CMOS recording time is 10 seconds. The recorded hologram is processed by PC to obtain a spectrogram and a reproduced image as shown in Fig. 11(a) and (b).The frequency domain 3D display and the corresponding reconstruction image's section line diagram are shown in Fig. 11(c) and (d).

Compared with the original spectrum Fig. 7 (a), the zero order term in the spectrum after temporal domain depolarization has been weakened to a large extent, and the interference to the object term has been very small. From the three-dimensional visualization of spectrum in Fig. 11 (c) and Fig.7 (a), it can also be seen intuitively that the temporal domain depolarization can significantly reduce the crosstalk of the three parts in the frequency domain. Compared with the original reconstruction Fig 7 (b), the speckle noise in the temporal domain depolarized reconstruction image is well suppressed, which greatly improves the overall quality of the image. It can be seen from section line Fig 11 (d) and Fig 8 (c) that it is almost difficult to distinguish the light and shade changes of the image from the section line figure of the original reconstruction map, while the section line figure of the temporal domain depolarization reconstruction map well reflects the edge information of the object itself. The calculated *ENL* is 0.7307, which is much lower than the original 0.9998. It just accords with the noise reduction model of the experimental system, and also confirms the accuracy of the experimental results.

Compared with spatial depolarization, the effect of spectrum Fig 11 (a) and figure 6 (c) is almost the same, both of them can suppress the interference of zero order term to object information. Furthermore, compared with the three-dimensional visualizations of spectrum Fig 11 (c), Fig 8 (a) and (b), the temporal domain depolarization not only suppresses the interference of the zero level term, but also has a small impact on the frequency-domain information of the object term, while the space domain depolarization suppresses the interference of the zero level term, at the same time, it also suppresses the frequency-domain information of the object term. This is because the temporal domain depolarization is the overall homogenization in time, which makes the incident linearly polarized light depolarize, and the polarization state of the outgoing light changes uniformly; while the spatial domain depolarization is the random depolarization of the linearly polarized light of different micro elements in space, and the outgoing light is obtained by the superposition of some random polarization states, so the overall uniformity is poor. This may lead to the lack of information of hologram obtained by spatial depolarization compared with that of temporal depolarization.

It can also be seen from Fig. 11 (b) and Fig. 7 (d) that the reconstructed image in Fig. 11 (b) is very smooth while speckle is suppressed. While the reconstruction image in Fig. 7 (d) suppresses the speckle, the uneven spot appears in the image. From the comparison of *ENL* between the two, *ENL* of Fig 11 (b) is 0.7307 and Fig 6 (c) is 0.7204. It is because of the contribution of dark spots in the spatial depolarization reconstruction that the calculated value of *ENL* is better. Compared with Fig 8 (d) and Fig 11 (d). All of them can distinguish the edge information of the object, while Fig 11 (d) has a smoother change in the pixel value of the information part of the object, while Fig 8 (d) has more abrupt changes. Therefore, on the whole, the details of time domain depolarization denoising are better preserved.

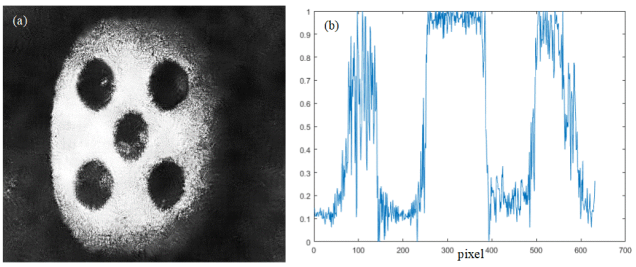

FIGURE 12. (a) Reconstructed image after NLM denoising and (b) is normalized values as in the same line position as in Fig. 7.

In order to verify the effectiveness of the two schemes in reducing speckle artifacts, the speckle contrast value is used to quantify the measured speckle [20]. Speckle contrast is determined by

$$\mathrm{SC} = \frac{\sigma}{\langle I \rangle} \tag{16}$$

Where $\langle I \rangle$ and σ represent the average values of the intensity and standard deviation of the captured image, respectively. The speckle contrast of the original reconstruction image Fig.7 (b) is 63.9%, The speckle contrast of the reconstructed image Fig7. (d) obtained by spatial depolarization is 49.8% and the speckle contrast of the reconstructed image Fig.11 (b) obtained by time domain depolarization is 46.6%. Therefore, the effectiveness of the two schemes can be proved by the reduction of speckle contrast.

Next, image processing algorithm is used to further denoise Fig. 11(b), and Non-Local Means(NLM) denoising is used. The result of processing is shown in Fig. 12(a). Compared with the processed Fig. 11(b), the speckle noise can be better suppressed and the image can be displayed more smoothly. At the same time, the normalized values graph of sectional pixel is shown in Fig.12(b). Compared with Fig. 10(d), it can be seen that the edge information is more obvious, and the pixels of the object information part are relatively more continuous, which shows that the reconstructed image has higher smoothness.

IV. CONCLUSION

In general, adding a quartz depolarizer to the object light path changes the polarization state for the outgoing beam of object light in the spatial, thereby reducing the effect on the degree of coherence for the object reference, thereby reducing speckle noise and improving image quality. The spatial depolarization method has compact structure, easy to implement, and highly cost-effective, and is suitable for traditional digital holographic structures. Moreover, it only needs to perform micro-displacement on the quartz depolarizer to realize the function of adjusting the degree of coherence, which is suitable for object shooting of different materials. On the other hand, by adding the quarter-wave plate and the change of the polarization state for the liquid crystal generation time, the hologram of multi-state interference is recorded, which can reduce the coherence degree and reduce the noise, and record more object information in different polarization states. The temporal domain depolarization method does not require additional mechanical operations, and records a large amount of information and has good stability. From the experimental results, it can be concluded that compared with the traditional digital holographic structure, the two structural schemes significantly reduce the speckle noise, and the temporal domain depolarization reserves the object details better. In the next work, we will study the effect of using USAF test pattern images on the minimum resolution, so that researchers can understand it more easily.

REFERENCES

[1] J. W. Goodman and W. Joseph, "Speckle phenomena in optics: Theory and applications," Tech. Rep., 2007.
[2] J. C. Dainty, *Laser Speckle and Related Phenomena*. New York, NY, USA: Springer-Verlag, 1984, p. 1533.
[3] T. Baumbach, E. Kolenovic, V. Kebbel, and W. Jüptner, "Improvement of accuracy in digital holography by use of multiple holograms," *Appl. Opt.*, vol. 45, no. 24, p. 6077, Aug. 2006.
[4] S. W. Hell and J. Wichmann, *Opt. Lett.*, vol. 19, pp. 780–782, 1984.
[5] Z. Liu, T. Gemma, J. Rosen, and M. Takeda, "An improved illumination system for spatial coherence control," *Appl. Opt.*, vol. 49, no. 16, pp. 12–16, 2010.
[6] T. Kreis, *Handbook of Holographic Interferometry: Optical and Digital Methods: Optical and Digital methods*. Weinheim, Germany: Wiley-VCH, 2005.
[7] C. Zuo, "Display and detail enhancement for high-dynamic-range infrared images," *Opt. Eng.*, vol. 50, no. 12, Dec. 2011, Art. no. 127401.
[8] T. Nomura, M. Okamura, E. Nitanai, and T. Numata, "Image quality improvement of digital holography by superposition of reconstructed images obtained by multiple wavelengths," *Appl. Opt.*, vol. 47, no. 19, p. D38, Jul. 2008.
[9] M. N. Morris, M. Naradikian, and J. Millerd, "Noise reduction in dynamic interferometry measurements," *Proc. SPIE*, vol. 7790, Aug. 2010, Art. no. 779000.
[10] M. Somekh, C. See, and J. Goh, "Wide field amplitude and phase confocal microscope with speckle illumination," *Opt. Commun.*, vol. 174, nos. 1–4, pp. 75–80, Jan. 2000.
[11] M. Tziraki, R. Jones, P. French, M. Melloch, and D. Nolte, "Photorefractive holography for imaging through turbid media using low coherence light," *Appl. Phys. B, Lasers Opt.*, vol. 70, no. 1, pp. 151–154, Jan. 2000.
[12] K. Badizadegan, *Speckle-Field Digital Holographic Microscopy*. New York, NY, USA: Springer, 2009.
[13] J. Garcia-Sucerquia, J. A. H. Ramírez, and D. V. Prieto, "Reduction of speckle noise in digital holography by using digital image processing," *Optik*, vol. 116, no. 1, pp. 44–48, Mar. 2005.
[14] Y. Takaki and M. Yokouchi, "Speckle-free and grayscale hologram reconstruction using time-multiplexing technique," *Opt. Express*, vol. 19, no. 8, p. 7567, Apr. 2011.
[15] M. Makowski, "Minimized speckle noise in lens-less holographic projection by pixel separation," *Opt. Express*, vol. 21, no. 24, Dec. 2013, Art. no. 29205.
[16] V. Bianco, P. Memmolo, M. Paturzo, and P. Ferraro, "On-speckle suppression in IR digital holography," *Opt. Lett.*, vol. 41, no. 22, pp. 5226–5229, 2016.
[17] Y. Zeng, J. Lu, X. Chang, Y. Liu, X. Hu, K. Su, and X. Chen, "A method to improve the imaging quality in dual-wavelength digital holographic microscopy," *Scanning*, vol. 2018, pp. 1–6, Oct. 2018.
[18] C. Shen, C. Guo, Y. Geng, J. Tan, S. Liu, and Z. Liu, "Noise-robust pixel-super-resolved multi-image phase retrieval with coherent illumination," *J. Opt.*, vol. 20, no. 11, Nov. 2018, Art. no. 115703.
[19] S. B. Ko, and J. H. Park, "Speckle reduction using angular spectrum interleaving for triangular mesh based computer generated hologram," *Opt. Express*, vol. 25, no. 24, 2017, Art. no. 29788.
[20] Y. Lim, J. Park, J. Hahn, H. Kim, K. Hong, and J. Kim, "Reducing speckle artifacts in digital holography through programmable filtration," *ETRI J.*, vol. 41, no. 1, pp. 32–41, 2019.

[21] D. S. Mehta, D. N. Naik, R. K. Singh, and M. Takeda, "Laser speckle reduction by multimode optical fibre bundle with combined temporal, spatial and angular diversity," *Appl. Opt.*, vol. 51, no. 12, pp. 1894–1904, 2012.
[22] W.-S. Ha, S.-J. Lee, K.-H. Oh, Y.-M. Jung, and J.-K. Kim, "Speckle reduction in near-field image of multimode fiber with a piezoelectric transducer," *J. Opt. Soc. Korea*, vol. 12, no. 3, pp. 126–130, Sep. 2008.
[23] A. L. Petoukhova, E. Cleven, F. F. M. De Mul, and W. Steenbergen, "Suppression of dynamic laser speckle signals in multimode fibers of various lengths," *Appl. Opt.*, vol. 43, no. 10, p. 2059, Apr. 2004.
[24] P. Georgiades, V. J. Allan, M. Dickinson, and T. A. Waigh, "Reduction of coherent artefacts in super-resolution fluorescence localisation microscopy," *J. Microscopy*, vol. 264, no. 3, pp. 375–383, Dec. 2016.
[25] V. Singh, R. Joshi, S. Tayal, D. S. Mehta, "Speckle-free common-path quantitative phase imaging with high temporal phase stability using a partially spatially coherent multi-spectral light source," *Laser Phys. Lett.*, vol. 16, no. 2, 2019, Art. no. 025601.
[26] S. Tayal, K. Usmani, V. Singh, V. Dubey, D. S. Mehta, "Speckle-free quantitative phase and amplitude imaging using common-path lateral shearing interference microscope with pseudo-thermal light source illumination," *Optik*, vol. 180, pp. 991–996, Feb. 2019.
[27] R. Hamdi, D. F. Bendimerad, B.-E. Benkelfat, and B. Vinouze, "Tuning of liquid-crystal birefringence using a square ac variable frequency voltage," *J. Opt.*, vol. 17, no. 10, Oct. 2015, Art. no. 105703.

TONGYAO DU received the B.S. degree from the Changzhou Institute of Technology, in 2017. He is currently pursuing the M.S. degree with the Shanghai University of Engineering Science. His research interests are digital holography and digital holography microscopy.

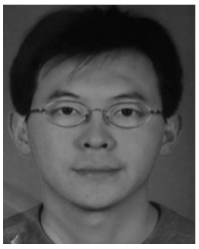

YONG KONG was born in May 1977. He received the Ph.D. degree in optics from the Shanghai Institute of Optics and Fine Mechanics, Chinese Academy of Sciences. He is currently with the Shanghai University of Engineering Science. His major research interests are optical fiber sensing and digital holography.

XINLEI QIAN received the B.S. degree from the Taihu College, in 2017. He is currently pursuing the M.S. degree with the Shanghai University of Engineering Science. His research interest includes digital holography for information processing.

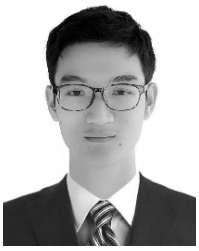

WEI DING received the B.S. degree from the Tongda College, Nanjing University of Posts and Telecommunications, in 2018. He is currently pursuing the M.S. degree with the Shanghai University of Engineering Science. His research interest is digital holography.

ZHENWEI WANG received the B.S. degree from Chuzhou University, in 2018. He is currently pursuing the M.S. degree with the Shanghai University of Engineering Science. His research interests are optical fiber sensing and digital holography.